AGU PUBLICATIONS

Geophysical Research Letters

RESEARCH LETTER

10.1002/2014GL059336

Key Points:
- With a Walker cell, the shortwave cloud feedback is reduced in the subtropics
- Suppressed feedback leads to weaker anomalous energy gradient
- Meridional energy gradient explains response of Hadley circulation under CO_2 increase

Correspondence to:
N. Feldl,
feldl@gps.caltech.edu

Citation:
Feldl, N., D. M. W. Frierson, and G. H. Roe (2014), The influence of regional feedbacks on circulation sensitivity, *Geophys. Res. Lett.*, *41*, doi:10.1002/2014GL059336.

Received 20 JAN 2014
Accepted 27 FEB 2014
Accepted article online 3 MAR 2014

The influence of regional feedbacks on circulation sensitivity

N. Feldl[1], D. M. W. Frierson[2], and G. H. Roe[3]

[1]Environmental Science and Engineering, California Institute of Technology, Pasadena, California, USA, [2]Department of Atmospheric Sciences, University of Washington, Seattle, Washington, USA, [3]Department of Earth and Space Sciences, University of Washington, Seattle, Washington, USA

Abstract Weakening of the tropical overturning circulation in a warmer world is a robust feature in climate models. Here an idealized representation of ocean heat flux drives a Walker cell in an aquaplanet simulation. A goal of the study is to assess the influence of the Walker circulation on the magnitude and structure of climate feedbacks, as well as to global sensitivity. We compare two CO_2 perturbation experiments, one with and one without a Walker circulation, to isolate the differences attributable to tropical circulation and associated zonal asymmetries. For an imposed Walker circulation, the subtropical shortwave cloud feedback is reduced, which manifests as a weaker tropical-subtropical anomalous energy gradient and consequently a weaker slow down of the Hadley circulation, relative to the case without a Walker circulation. By focusing on the coupled feedback circulation system, these results offer insights into understanding changes in atmospheric circulation and hence the hydrological cycle under global warming.

1. Introduction

An aquaplanet model provides a simplified framework for understanding how atmospheric feedbacks control regional patterns of climate change. Such simulations have proved useful for identifying both robust behaviors of the atmosphere as well as fundamental uncertainties in the response of clouds and precipitation [*Medeiros et al.*, 2008; *Stevens and Bony*, 2013; *Rose et al.*, 2014]. However, the feedbacks in an aquaplanet are, by the nature of the experimental setup, zonally symmetric. While this is an important first approximation to investigate, and may hold approximately in the middle and high latitudes, we expect and see striking zonal asymmetries in the tropics. In particular, the standard aquaplanet configuration does not capture the full expression of real-world atmospheric circulations and associated cloud response in the tropical Pacific.

Many of the Pacific asymmetries are linked to the Walker circulation, a tropical overturning circulation characterized by convection over the west Pacific warm pool and subsidence over the eastern Pacific. Variability in the Walker circulation is associated with El Niño–Southern Oscillation [*Bjerknes*, 1969; *Julian and Chervin*, 1978] and the Asian monsoon [*Webster et al.*, 1998]. Importantly, the Walker circulation represents a coupled system between ocean and atmosphere. The strength of equatorial Pacific wind stress in the lower branch of the Walker circulation induces changes in ocean circulation, thermocline depth, upwelling, and air-sea fluxes [*Xie*, 1998; *Xie et al.*, 2010; *Lu and Zhao*, 2012], which in turn feed back on the atmosphere.

Tropical circulation is anticipated to weaken under global warming. Two consistent arguments are proposed with analogs in the west and east Pacific, respectively. First, in regions of ascent, a smaller increase in global precipitation with warming (2%/K) relative to the increase in boundary layer water vapor (7%/K per Clausius-Clapeyron) implies a decrease in convective mass flux [*Betts*, 1998; *Held and Soden*, 2006]. Second, in regions of descent, a larger increase in dry stability relative to the radiative cooling of the troposphere implies a weakening of subsidence [*Knutson and Manabe*, 1995]—at the same rate as the convective mass flux argument of *Held and Soden* [2006]. By both metrics, then, the overturning atmospheric circulation weakens as the climate warms. This weakening is a robust result in general circulation models (GCM) [*Vecchi and Soden*, 2007] and observations [*Vecchi et al.*, 2006]. Though the zonally asymmetric (i.e., Walker) component exhibits a stronger signal, the zonally symmetric (i.e., Hadley) component is also projected to weaken [*Held and Soden*, 2006; *Lu et al.*, 2007].

The strength of the tropical overturning circulation affects the persistence of radiatively important low clouds in the eastern Pacific [e.g., *Bony et al.*, 2004]. The Walker circulation is thus implicated in driving changes in cloud cover that are thought to provide the largest source of uncertainty in model estimates of climate sensitivity to increased greenhouse gases [*Colman*, 2003; *Soden and Held*, 2006; *Webb et al.*, 2006].

Soden and Vecchi [2011] show that for a suite of GCMs, the individual members exhibit high variability in cloud feedback with large zonal asymmetries across the tropical Pacific. However, many of these features are averaged out in the ensemble mean, which is characterized by a positive high cloud feedback in the longwave, consistent with the tendency of tropical anvils to conserve cloud top temperature [*Zelinka and Hartmann*, 2010], and offsetting shortwave feedback. Understanding the coupling between clouds and circulation is central to the accurate representation of climate feedbacks in models.

Zonal asymmetries are not a general feature of the aquaplanet, and yet they are clearly fundamental to more complex models, as well as to nature. A goal of this study is to assess the influence of the Walker circulation on the magnitude and structure of feedbacks, as well as to global sensitivity. We apply an incremental approach and compare two aquaplanet simulations, one with and one without a Walker circulation, in order to isolate the portion of differences that can be cleanly attributed to tropical circulation. We are further motivated to investigate whether feedbacks may in turn offer insights into understanding changes in atmospheric circulation under global warning.

2. The Walker Aquaplanet

We employ the Geophysical Fluid Dynamics Laboratory Atmospheric Model 2.1 [*Delworth et al.*, 2006] in its aquaplanet configuration with perpetual equinox and daily mean solar zenith angle. The ocean is represented as a 20 m mixed layer. Sea ice is treated as infinitesimally thin; the ocean albedo is increased to 0.5 where surface temperature drops below 263 K, but the model has no representation of ice thermodynamics. The critical temperature for sea ice formation was chosen to reproduce a realistic ice line latitude, when compared to the modern climate. Our perturbation is achieved by an instantaneous doubling of CO_2, followed by integration to equilibrium. The idealized configuration allows us to isolate the physics and dynamics of the atmospheric response to CO_2 in the absence of land-surface processes and seasonal and diurnal cycles. The limitations of these simplifications are discussed in section 5.

A prescribed ocean heat flux divergence is applied to the ocean surface to generate a zonal overturning circulation in the tropics. The specified ocean heat fluxes (commonly referred to as "q-flux") are constant in time, and they represent the influence of ocean circulation on the surface temperature. The q-flux is given by the following equation, modified from *Merlis and Schneider* [2011]. Gaussian lobes of positive and negative divergence are positioned on the equator at longitudes λ_E and λ_W:

$$\nabla \cdot F_O(\lambda,\phi) = Q_1 \exp\left[-\frac{(\lambda-\lambda_E)^2}{\lambda_1^2}-\frac{\phi^2}{\phi_1^2}\right] - Q_1 \exp\left[-\frac{(\lambda-\lambda_W)^2}{\lambda_1^2}-\frac{\phi^2}{\phi_1^2}\right] \quad (1)$$

where ϕ is latitude and $\phi_1 = 7°$; λ is longitude and $\lambda_1 = 30°$, $\lambda_E = 120°$, and $\lambda_W = 270°$. $Q_1 = 75\ \mathrm{W\ m^{-2}}$, which is the peak magnitude of the anomalies. The resulting q-flux is shown in Figure 1. It is zero in the global mean.

Figure 1c shows the control (i.e., 1 × CO_2) zonal mass stream function, averaged over the last 10 years of our 30 year integration. The aquaplanet exhibits both Hadley and Walker cells, and circulation strength is broadly consistent with observations [*Trenberth et al.*, 2000]. Ascent is focused over the positive ocean heat flux anomaly and descent over the negative heat flux anomaly, as expected. The distribution of clouds is consistent with these vertical motions. Upper level cloud fraction peaks at 200 hPa over the warm pool and reaches a minimum (at all levels) over the cold pool. The cloud feedback (discussed later) is a consequence of changes to the location and amount of these clouds, as well as their optical properties, for a doubling of CO_2. Near-surface winds indicate low-level convergence into the warm pool. Outgoing longwave radiation is reduced in regions of high clouds and increased in clear-sky regions, which occur over boundary layer clouds. The equatorial sea surface temperature (SST) gradient between the warm and cold ocean anomalies is 3 K.

We apply the radiative kernel method of calculating climate feedbacks, following *Soden and Held* [2006]. Feedbacks are computed by convolving the kernel ($\partial R/\partial x$, i.e., the top-of-atmosphere flux sensitivity to a small perturbation in climate variable x) with 10 years of equilibrated monthly anomalies, dx (2 × CO_2 minus

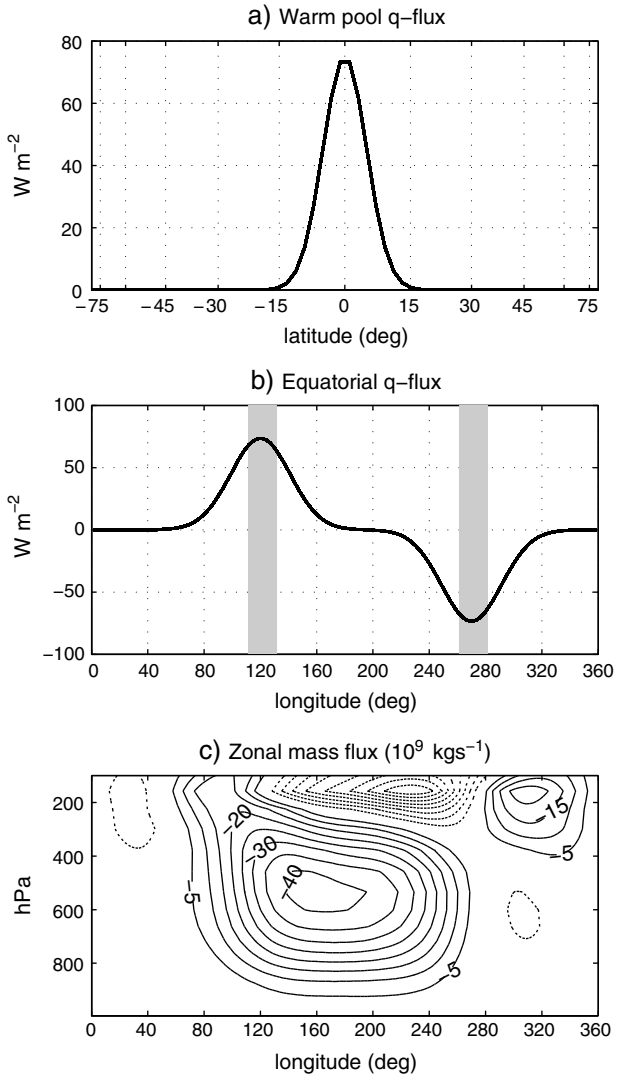

Figure 1. Ocean heat flux convergence, q-flux, in W m^{-2} (a) at the longitude of the warm pool and (b) at the equator. Positive values indicate warming tendencies. The western anomaly is located to coincide with the real-world west Pacific warm pool, the eastern anomaly, with the eastern Pacific cold tongue. (c) Zonal mass flux at the equator, induced by q-flux, for 1 × CO_2 climatology. Solid lines indicate clockwise flow. Contour interval is 5 × 10^9 kg s^{-2}.

1 × CO_2). The feedback is divided by the local near-surface air temperature response, ΔT_s, to give units of W m^{-2} K^{-1};

$$\lambda_x = \frac{\partial R}{\partial x}\frac{dx}{\Delta T_s} \tag{2}$$

where x represents temperature, specific humidity, or surface albedo. A more common approach is to divide by the global mean surface temperature change, $\Delta\overline{T_s}$; however, as *Feldl and Roe* [2013a] discuss, the local definition offers a number of advantages when regional patterns of climate change are of interest.

A strength of our analysis is that we explicitly calculate radiative kernels for our precise Walker aquaplanet experimental setup. To create the kernel, small perturbations are applied independently to the temperature (T), water vapor (q), and surface albedo (α) fields of the 1 × CO_2 simulation, and their effects on the top-of-atmosphere (TOA) radiative flux are calculated. The kernels we derive resemble the kernels calculated from the aquaplanet of *Feldl and Roe* [2013b] (used in the symmetric calculations herein) but with zonal asymmetries due to the inclusion of a Walker circulation, which affect the tropospheric structure in the tropics.

The cloud feedback cannot be simply calculated using radiative kernels, due to nonlinearities associated with their complex spatial structure. Following *Soden et al.* [2008], we compute the cloud feedback, λ_c, from the change in cloud radiative effect, ΔCRF, with adjustments for cloud masking:

$$\lambda_c \Delta T_s = \Delta\mathrm{CRF} + (K_T^0 - K_T)dT + (K_q^0 - K_q)dq + (K_\alpha^0 - K_\alpha)d\alpha + (\Delta R_f^0 - \Delta R_f) \tag{3}$$

where K^0 terms are the clear-sky kernels, ΔR_f^0 is the clear-sky forcing, and ΔCRF is defined as the difference between net downward radiative fluxes in all-sky (i.e., the observed meteorological conditions, including clouds if present) and clear-sky (i.e., assuming no cloud) conditions. The additional cloud masking terms are needed because the presence of clouds modifies the TOA fluxes due to underlying lapse rate, water vapor, surface albedo, and CO_2 [*Soden et al.*, 2004].

Radiative forcing due to the CO_2 perturbation enters in equation (3), and there are choices to be made here as well. Three common metrics are stratosphere-adjusted forcing, fixed SST (or troposphere-adjusted) forcing, and a constant, global mean value. The radiative forcing should represent any TOA flux changes after introduction of the forcing agent but before surface temperature change, i.e., cleanly separating forcing from feedback. While the fixed SST radiative forcing may be preferred because it accounts for rapid cloud responses directly to CO_2 [*Colman and McAvaney*, 2011; *Andrews et al.*, 2011], it is a noisy calculation with

Table 1. Global Mean, Annual Mean Feedbacks for Aquaplanet Simulations With (Top Row) and Without (Bottom Row) Walker Circulations[a]

	P	LR	WV	A	Net Cloud	LW Cloud	SW Cloud	Net	Residual
Walker	−3.03	−0.53	1.46	0.34	1.15	0.38	0.77	−0.61	−0.16
Symmetric	−3.03	−0.69	1.62	0.35	1.33	0.49	0.83	−0.43	−0.31

[a]Planck (P), lapse rate (LR) plus water vapor (WV), and albedo (A) feedbacks are strikingly similar. The net feedback is the sum of the linear feedbacks. The residual in the local energy balance is interpreted as the nonlinear term. Units are W m^{-2} K^{-1}. In both cases a stratosphere-adjusted estimate of radiative forcing is used ($\Delta\overline{R_f} = 3.4$ W m^{-2}). Note that the global mean of globally defined feedbacks presented in this table differs from the global mean of the locally defined feedbacks of Figure 2 by a factor of $\Delta T_s(\phi)/\Delta\overline{T_s}$.

high spatial and temporal variability. Here we use a stratosphere-adjusted radiative forcing [*Ramaswamy et al.*, 2001; *Hansen et al.*, 2005] derived from the basic aquaplanet without a Walker circulation; stratospheric changes are expected to be comparable between the experiments. The global mean value is 3.4 W m^{-2}. As *Feldl and Roe* [2013b] show, the choice between the two aquaplanet-derived forcings has only a minor effect on the feedback analysis for this model setup.

3. Atmospheric Feedbacks and Transport

Climate sensitivity is remarkably similar between the two experiments, in spite of the very different patterns of tropical circulation. The symmetric (i.e., no q-flux) experiment has an equilibrium climate sensitivity of 4.8 K and a net feedback parameter of −0.43 W m^{-2} K^{-1}. For the Walker experiment, we find values of 4.5 K and −0.61 W m^{-2} K^{-1}, respectively (Table 1). As expected, global mean surface temperature change is reduced given a more negative net feedback. However, if we were to estimate climate sensitivity assuming linearly independent feedbacks (i.e., $\Delta\overline{T_s} = \Delta\overline{R_f}/\overline{\sum \lambda_x}$), then we would anticipate a larger difference (30%). The reason we find only a 6% reduction in sensitivity is that the residual nonlinear term (right-hand column) is halved. Thus, the doubling of CO_2 leads to considerable warming when a Walker circulation is present, even though the feedback is more stabilizing, because of increased linearity. The nonlinearity is explained by *Feldl and Roe* [2013b] as due to interactions among feedbacks, including clear-sky masking.

Global mean feedbacks are presented in Table 1 for the Walker and symmetric aquaplanets. The temperature feedback is strongly negative: A warmer planet emits more radiation to space (Planck feedback), and the weakened lapse rate, which is a consequence of moist adiabatic stratification, leads to emission from a warmer atmosphere than if lapse rate were fixed (lapse rate feedback). The water vapor feedback is strongly positive because humidity is highly sensitive to warming and because moistening the atmosphere increases infrared opacity and downwelling radiation. The surface albedo feedback is positive and controlled by sea ice processes in this model. In general, the longwave (LW) cloud feedback is associated with the role of clouds in reducing emission, and the shortwave (SW) cloud feedback is associated with the role of clouds in increasing planetary albedo (i.e., a positive SW cloud feedback indicates a decrease in reflectivity). The effect of a particular cloud on the energy balance depends strongly on its height and optical thickness.

The Planck, surface albedo, and combined water vapor plus lapse rate feedbacks are unchanged between the two experiments. However, the cloud feedback is weaker (less positive) in the Walker aquaplanet, preferentially due to changes in the longwave component. To identify the source of the differences in cloud response, we turn to the spatial structure of the aquaplanet feedbacks. As in the global mean, the zonal mean net feedback is weaker in the Walker aquaplanet relative to the symmetric aquaplanet (Figures 2a and 2b, black line). The largest differences occur in the subtropics, associated with cloud and water vapor feedbacks, hinting at the role of the zonal circulation in modulating the meridional circulation. We expect to see a large water vapor feedback, for instance, where strongly suppressed subtropical descent leads to anomalous moistening. North-south hemispheric asymmetries in Figure 2 are due to internal model variability.

The distinct features of the Walker aquaplanet feedbacks are associated with the presence of the imposed warm and cold pools at the equator (Figures 2c and 2d). The net feedback (black line) exhibits striking zonal asymmetries in the tropics and subtropics—in particular, a negative feedback over the cold pool where the Intertropical Convergence Zone is suppressed and equatorial precipitation minimized. This behavior is mirrored in the cloud feedback (blue line). The cold pool is characterized by a broad region of negative longwave cloud feedback (Figure 2g, purple line) and a weakening of the positive shortwave cloud feedback

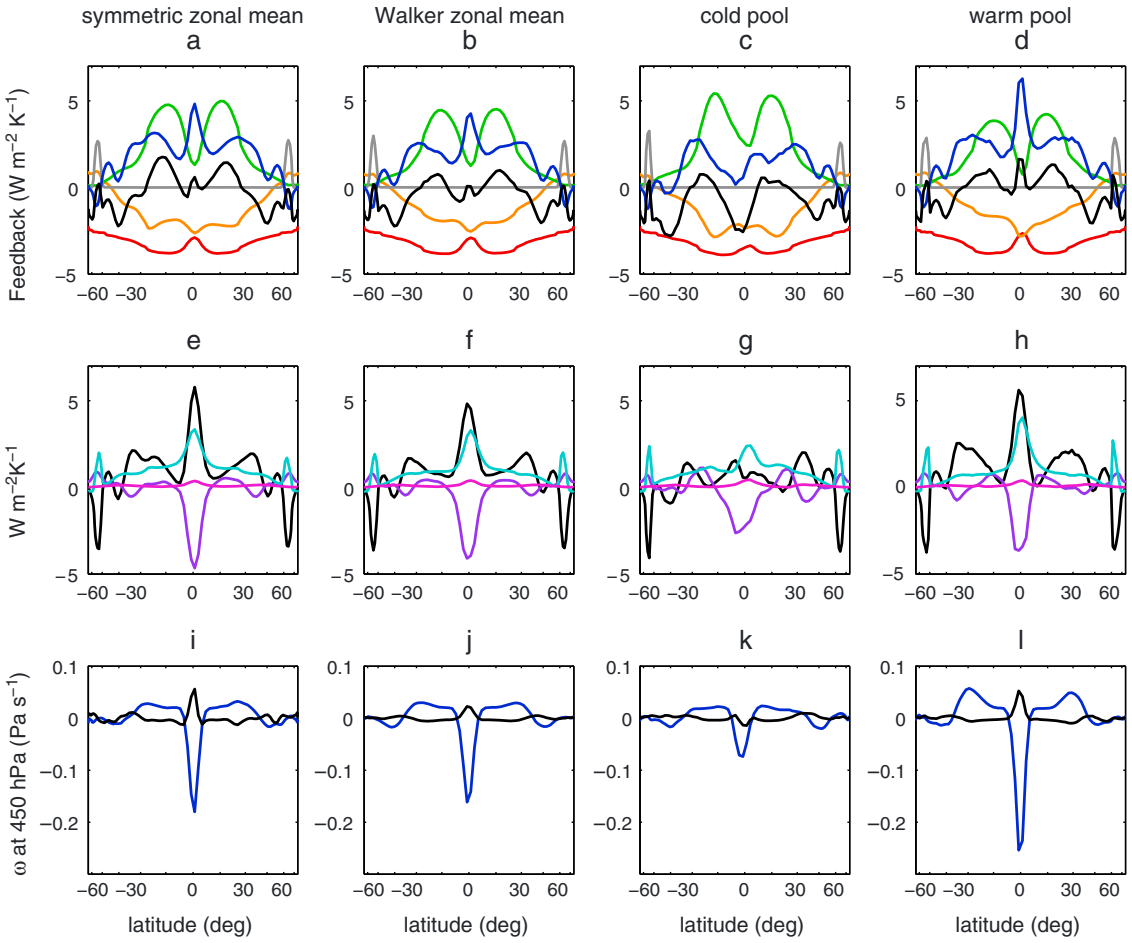

Figure 2. (a–d) Annual mean (W m^{-2} K^{-1}) Planck (red), lapse rate (orange), water vapor (green), surface albedo (gray), cloud (blue), and net feedbacks (black) for the zonal mean and at longitude bands specified in Figure 1b. (e–h) Components of cloud feedback, ΔCRF for SW (black) and LW (purple), masking terms (cyan), and forcing correction (magenta). (i–l) Midtropospheric vertical pressure velocity, ω (Pa s^{-1}), in the $1\times CO_2$ climate (blue) and $2\times CO_2$ minus $1\times CO_2$ anomalies (black).

along the equator (black line). The remaining feedbacks in Figures 2c and 2d are more zonally symmetric, though the water vapor feedback (green line) is enhanced on the subtropical flanks of the cold pool. Interestingly, while the deep tropics exhibit remarkable cancellation between positive and negative feedback at the warm and cold pool, such that it resembles the symmetric zonal mean, there is no such cancellation in the subtropics.

Cloud changes are consistent with the structure of the cloud feedback and result from the interplay of suppressed ascent and descent in both the zonal and meridional components of tropical circulation. In our simulations, the Walker circulation weakens by 45% and the Hadley circulation by 15% under CO_2 doubling. By comparison, coupled model studies report 5–10% K^{-1} [*Vecchi and Soden*, 2007] and 0–4% K^{-1} [*Lu et al.*, 2007], respectively, which roughly converts to 22–45% and 0–18% for our climate sensitivity. This tendency of overturning circulation to weaken is also apparent in midtropospheric vertical velocity in pressure coordinates, ω (Figures 2i–2l). A decrease in ascent at the equator is indicated by a positive anomalous vertical velocity (black line) and is largest at the warm pool and in the symmetric zonal mean. Accordingly, these regions see decreases in cloud fraction aloft, by up to 15%, that are consistent with the negative longwave cloud feedback and the compensating positive shortwave cloud feedback. Upper level cloud changes at the cold pool—where high clouds are thinner to start—are smaller but also more spatially extensive (Figure 3, bottom right).

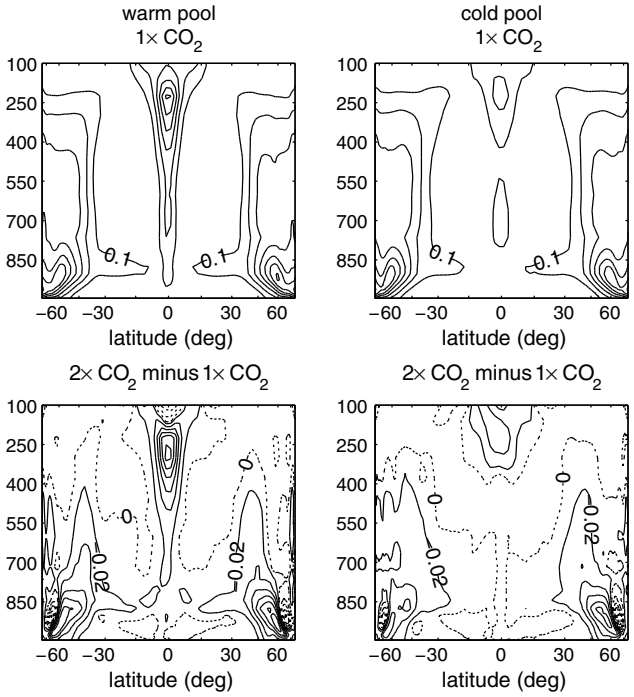

Figure 3. (top row) Cloud fraction climatology (contour interval, 0.1) and (bottom row) change (contour interval, 0.03) at the longitude bands specified in Figure 1b. Decreases in cloud fraction, consistent with a positive SW cloud feedback, are indicated by solid lines.

4. Some Longitudes are Less Cloudy

By adding a Walker circulation, we disrupt the symmetry of the Hadley circulation and introduce broad regions of negative cloud feedback near the equatorial cold pool. This feedback lowers the net feedback, both locally and in the zonal mean. Since anomalous energy transport is directed away from regions of net positive feedback, the gradient of cloudiness will play an important role in the climate response. With one notable exception, midlevel cloud fraction at all but the highest latitudes decreases under CO_2 doubling, with largest changes at 30°. This cloud response manifests as a positive SW ΔCRF (Figures 2e–2h, black line) and negative LW ΔCRF (purple line) and is consistent with a reduction in strength of the meridional circulation. The exception is at the cold pool, where another process is superimposed on the weakening of the Hadley circulation: the Walker circulation also weakens. Competing circulation tendencies at the ascending branch of the Hadley circulation and descending branch of the Walker circulation largely cancel at the equatorial cold pool (Figure 2k, black line). In particular, where the tropical high clouds are thinner to start, the cloud changes are also much smaller under CO_2 doubling. Consequently, the SW cloud effect essentially disappears over the cold pool (Figure 2g), the LW effect dominates the ΔCRF, the cloud feedback is neutral, and the net feedback, negative (Figure 2c).

In addition to the near-zero tropical cloud feedback at the cold pool, the magnitude of the subtropical cloud feedback is also reduced, which affects the zonal mean (Figures 2a and 2b). Consequently, the *gradient* of the net feedback across the subtropics is weaker in the Walker aquaplanet compared to the symmetric aquaplanet. As in the case of tropical high clouds, both the climatological cloudiness and cloud changes at 850 hPa are smaller at the longitude of the cold pool (Figure 3). Because the induced cold pool is a heat sink, weaker vertical motions lead to more uniform cloud cover across the tropics and subtropics. In contrast, the warm pool produces a stronger gradient in cloudiness and a stronger gradient in SW ΔCRF, cloud feedback, and net feedback. Climatologically, the warm pool with its vigorous Hadley circulation bears more similarity to the symmetric aquaplanet (Figures 2h and 2e). It is also of note that the cloud masking terms (Figure 2e, cyan line), which are derived from the 1 × CO_2 kernels, contribute to the stronger subtropical cloud feedback in the symmetric aquaplanet. At 15°, for instance, both SW ΔCRF and the masking terms are larger in the symmetric aquaplanet, compared to the Walker aquaplanet (Figures 2e and 2f), accounting for the difference in feedback gradient.

We now turn to the Hadley cell response under global warming (Figures 2i and 2j). The zonal mean, climatological meridional circulation (blue lines) is strikingly similar between the Walker and symmetric aquaplanets. However, the response of the circulation under doubling of CO_2 (black lines) is different: The Walker aquaplanet exhibits a weaker slow down (14.9%), which is explained by the weaker subtropical feedback gradient. The symmetric case has a stronger feedback gradient and consequently a stronger reduction in circulation (16.7%) (Circulation intensity is calculated as the difference between the extrema of the meridional mass stream function below 100 hPa.). A positive feedback represents a region of anomalous divergence of atmospheric heat flux, since the TOA fluxes are not efficiently accommodating energy perturbations. Likewise for negative feedback and anomalous convergence. Thus, the stronger the feedback

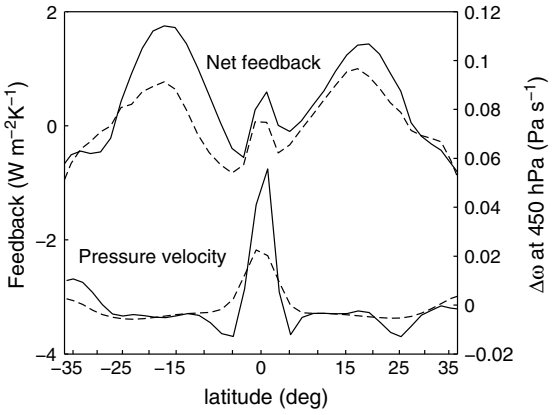

Figure 4. Annual mean low-latitude feedback (W m^{-2} K^{-1}) and change in midtropospheric vertical pressure velocity, ω (Pa s^{-1}), for the Walker (dashed) and symmetric (solid) aquaplanet simulations. Curves reproduced from Figure 2.

gradient, the more anomalous the heat transport from subtropics to the tropics (i.e., the larger the decrease in tropical heat export). The primary way the atmosphere modulates tropical energy transports is by changing the intensity of the meridional circulation [*Kang et al.*, 2008]. We emphasize that because the zonal mean climatological circulation is quite similar between the two experiments, the feedbacks are specifically affecting the *sensitivity* of the circulation response. In other words, while the climatological circulation sets the pattern of feedbacks, it is the feedbacks that drive the circulation response.

5. Summary and Discussion

In this study, we characterize the effect of zonal circulation asymmetries upon climate feedbacks. We have designed an experiment that takes advantage of simplified, aquaplanet boundary conditions, paired with a full-complexity atmospheric GCM. Our climate sensitivity is reduced—from 4.8 K to 4.5 K—as a consequence of the Walker circulation, and this reduction is consistent with broad regions of negative feedback in the vicinity of the imposed cold pool. The role of the Walker circulation is to suppress the cloud feedback and enhance the water vapor feedback at the longitude of the cold pool, though the latter is compensated by an enhancement of the negative lapse rate feedback. The pattern of the cold pool cloud feedback is consistent with (1) minimal circulation changes and (2) uniformly less cloud cover. In particular, the strongly positive SW cloud feedback is suppressed at the longitude of the cold pool, due to only small decreases in tropical clouds aloft and subtropical clouds at low levels.

As a consequence of this weakly positive feedback on the subtropical flanks of the cold pool, the zonal mean feedback gradient is weaker in the Walker aquaplanet (Figure 4). This places an energetic requirement on the response of the tropical circulation, predicting a weaker slow down of the Hadley cell under CO_2 doubling, compared to the symmetric aquaplanet. The radiative warming tendency in the subtropics (due to cloud and water vapor feedbacks) is balanced by dynamical cooling (weakening of descent, i.e., less adiabatic warming) and the tropical radiative cooling tendency by weakening ascent. In the case of a stronger energetic gradient between the subtropics and tropics, these responses will be correspondingly stronger, as is born out in our experiments. Thus, regional feedbacks not only describe the radiative response to an imposed forcing but also couple meaningfully to circulation changes. Because the feedback can be expressed in terms of particular pieces of physics (water vapor, clouds, etc.), this work offers insights for understanding the drivers of dynamical changes under global warming.

The Walker circulation alone appears to be insufficient to substantially alter global climate sensitivity in our model. However, the differing circulation responses may shed some light on the increased linearity in the Walker aquaplanet. In regions of strong moistening, we expect a larger nonlinearity [*Feldl and Roe*, 2013b]. This leads to two expectations: that the nonlinearity should display a peak in magnitude in the subtropics, associated with a decrease in circulation intensity and relative moistening, and that the nonlinearity should be smaller in the Walker case, because a weaker slow down requires relatively less moistening. Both are observed, and future work will pursue the hypothesis that modest moistening (perhaps associated with increased model realism) may be a requirement of the linear feedback assumption.

By integrating experiments with and without the simulated Walker circulation, a strength of this study is that we isolate the effect of zonal circulation on feedbacks. However, a few caveats bear mention. First, while aquaplanets capture a number of robust responses of the large-scale circulation and hydrological cycle to warming, our simplifying assumptions do remove many of the key components of a realistic tropical Pacific circulation. Land-sea contrast is expected to have a profound effect on boundary layer cloud climatology, and the presence of continents also influences the midlatitude eddies that in turn interact with the meridional overturning circulation. Moreover, convective parametrizations within GCMs are affected

by the diurnal cycle, which we preclude by specifying a daily mean solar zenith angle. Future work will incrementally add complexity.

A second caveat is that a slab ocean model with specified, and static, ocean heat transport does not realistically represent ocean-atmosphere interactions. An understanding of the role of dynamical ocean adjustments in the surface warming response remains elusive, and a number of coupled mechanisms have been proposed. *Vecchi and Soden* [2007] find that in coupled models, the western Pacific shoals due to a weakening of equatorial easterlies and that this shoaling leads to warming of surface waters—a negative feedback on the strength of the Walker circulation. Hence, the atmospheric circulation weakens *more* in slab ocean models, compared to fully coupled models, indicating that ocean dynamics are not of primary importance. Specifically, *Lu and Zhao* [2012] suggest that the wind-evaporation-SST feedback (under which a strengthening of near-surface wind decreases SST through enhanced evaporation) is the dominant mechanism affecting tropical SST patterns. In our aquaplanet simulation, we are unable to characterize the extent to which coupled ocean-atmosphere processes modify the picture of regional climate change.

We have extended the climate feedback framework to consider the effect of ocean heat transport and associated atmospheric circulation changes. In many ways, the Walker aquaplanet is quite similar to its symmetric counterpart, with an overall symmetric pattern of warming. That is, strong regional feedbacks are set by the climatological circulation, and the atmosphere redistributes heat such that the patterns of warming remain remarkably uniform. In the tropics this is consistent with an efficient global circulation that eliminates dynamical gradients. From the feedback perspective, the climate system tends to allocate energy toward regions that can most effectively radiate to space, and our small reduction in global sensitivity appears to be a consequence of this effect: by punching a hole in tropical convergence zone clouds in the mean state, we slightly increase the Earth's ability to cool itself. Thus, sensitivity is controlled by both climatology and dynamics, and comparison of the aquaplanet with and without a Walker circulation suggests that shrinking the area of negative feedback will lead to enhanced sensitivity.

Acknowledgments
We thank David Battisti and Simona Bordoni for discussions, two anonymous reviewers for helpful comments, and the editor. N.F. was supported by the Foster and Coco Stanback Postdoctoral Fellowship.

The Editor thanks Alexandra Jonko and an anonymous reviewer for their assistance in evaluating this paper.

References

Andrews, T., J. M. Gregory, P. M. Forster, and M. J. Webb (2011), Cloud adjustment and its role in CO_2 radiative forcing and climate sensitivity: A review, *Surv. Geophys.*, *33*(3-4), 619–635, doi:10.1007/s10712-011-9152-0.

Betts, A. K. (1998), Climate-convection feedback: Some further issues, *Clim. Change*, *39*, 35–38.

Bjerknes, J. (1969), Atmopsheric teleconnections from the equatorial Pacific, *Mon. Weather Rev.*, *97*(3), 163–172.

Bony, S., J. L. Dufresne, H. Le Treut, J. J. Morcrette, and C. Senior (2004), On dynamic and thermodynamic components of cloud changes, *Clim. Dyn.*, *22*, 71–86, doi:10.1007/s00382-003-0369-6.

Colman, R. A. (2003), A comparison of climate feedbacks in general circulation models, *Clim. Dyn.*, *20*, 865–873, doi:10.1007/s00382-003-0310-z.

Colman, R. A., and B. McAvaney (2011), On tropospheric adjustment to forcing and climate feedbacks, *Clim. Dyn.*, *36*(9), 1649–1658.

Delworth, T. L., et al. (2006), GFDL's CM2 global coupled climate models: Part I. Formulation and simulation characteristics, *J. Clim.*, *19*(5), 643–674, doi:10.1175/JCLI3629.1.

Feldl, N., and G. H. Roe (2013a), Four perspectives on climate feedbacks, *Geophys. Res. Lett.*, *40*, 4007–4011, doi:10.1002/grl.50711.

Feldl, N., and G. H. Roe (2013b), The nonlinear and nonlocal nature of climate feedbacks, *J. Clim.*, *26*, 8289–8304, doi:10.1175/JCLI-D-12-00631.1.

Hansen, J., et al. (2005), Efficacy of climate forcings, *J. Geophys. Res.*, *110*, D18104, doi:10.1029/2005JD005776.

Held, I. M., and B. J. Soden (2006), Robust responses of the hydrological cycle to global warming, *J. Clim.*, *19*(21), 5686–5699, doi:10.1175/JCLI3990.1.

Julian, P. R., and R. M. Chervin (1978), A study of the Southern Oscillation and Walker circulation phenomenon, *Mon. Weather Rev.*, *106*(10), 1433–1451.

Kang, S. M., I. M. Held, D. M. W. Frierson, and M. Zhao (2008), The response of the ITCZ to extratropical thermal forcing: Idealized slab-ocean experiments with a GCM, *J. Clim.*, *21*(14), 3521–3532, doi:10.1175/2007JCLI2146.1.

Knutson, T. R., and S. Manabe (1995), Time-mean response over the tropical pacific to increased CO_2 in a coupled ocean-atmosphere model, *J. Clim.*, *8*(9), 2181–2199.

Lu, J., and B. Zhao (2012), The role of oceanic feedback in the climate response to doubling CO_2, *J. Clim.*, *25*(21), 7544–7563, doi:10.1175/JCLI-D-11-00712.1.

Lu, J., G. A. Vecchi, and T. Reichler (2007), Expansion of the Hadley cell under global warming, *Geophys. Res. Lett.*, *34*, L06805, doi:10.1029/2006GL028443.

Medeiros, B., B. Stevens, I. M. Held, M. Zhao, D. L. Williamson, J. G. Olson, and C. S. Bretherton (2008), Aquaplanets, climate sensitivity, and low clouds, *J. Clim.*, *21*(19), 4974–4991, doi:10.1175/2008JCLI1995.1.

Merlis, T. M., and T. Schneider (2011), Changes in zonal surface temperature gradients and Walker circulations in a wide range of climates, *J. Clim.*, *24*, 4757–4768, doi:10.1175/2011JCLI4042.1.

Ramaswamy, V., et al. (2001), Radiative forcing of climate change, in *Climate Change 2001: The Scientific Basis. Contribution of Working Group I to the Third Assessment Report of the Intergovernmental Panel on Climate Change*, edited by J. T. Houghton, et al., pp. 881, Cambridge Univ. Press, Cambridge, U. K., and New York.

Rose, B. E. J., K. C. Armour, D. S. Battisti, N. Feldl, and D. D. B. Koll (2014), The dependence of transient climate sensitivity and radiative feedbacks on the spatial pattern of ocean heat uptake, *Geophys. Res. Lett.*, *41*, doi:10.1002/2013GL058955.

Soden, B. J., and I. M. Held (2006), An assessment of climate feedbacks in coupled ocean–atmosphere models, *J. Clim.*, *19*(14), 3354–3360, doi:10.1175/JCLI3799.1.

Soden, B. J., and G. A. Vecchi (2011), The vertical distribution of cloud feedback in coupled ocean-atmosphere models, *Geophys. Res. Lett.*, *38*, L12704, doi:10.1029/2011GL047632.

Soden, B. J., A. J. Broccoli, and R. S. Hemler (2004), On the use of cloud forcing to estimate cloud feedback, *J. Clim.*, *17*(19), 3661–3665.

Soden, B. J., I. M. Held, R. Colman, K. M. Shell, J. T. Kiehl, and C. A. Shields (2008), Quantifying climate feedbacks using radiative kernels, *J. Clim.*, *21*(14), 3504–3520, doi:10.1175/2007JCLI2110.1.

Stevens, B., and S. Bony (2013), What are climate models missing?, *Science*, *340*(6136), 1053–1054.

Trenberth, K. E., D. P. Stepaniak, and J. M. Caron (2000), The global monsoon as seen through the divergent atmospheric circulation, *J. Clim.*, *22*, 3969–3993.

Vecchi, G. A., and B. J. Soden (2007), Global warming and the weakening of the tropical circulation, *J. Clim.*, *20*(17), 4316–4340.

Vecchi, G. A., B. J. Soden, A. T. Wittenberg, I. M. Held, A. Leetmaa, and M. J. Harrison (2006), Weakening of tropical pacific atmospheric circulation due to anthropogenic forcing, *Nature*, *441*(7089), 73–76.

Webb, M. J., et al. (2006), On the contribution of local feedback mechanisms to the range of climate sensitivity in two GCM ensembles, *Clim. Dyn.*, *27*(1), 17–38, doi:10.1007/s00382-006-0111-2.

Webster, P. J., V. O. Magaña, T. N. Palmer, J. Shukla, R. A. Tomas, M. Yanai, and T. Yasunari (1998), Monsoons: Processes, predictability, and the prospects for prediction, *J. Geophys. Res.*, *103*(C7), 14,451–14,510, doi:10.1029/97JC02719.

Xie, S.-P. (1998), Ocean–atmosphere interaction in the making of the Walker circulation and equatorial cold tongue, *J. Clim.*, *11*(2), 189–201.

Xie, S.-P., C. Deser, G. Vecchi, J. Ma, H. Teng, and A. Wittenberg (2010), Global warming pattern formation: Sea surface temperature and rainfall, *J. Clim.*, *23*, 966–986.

Zelinka, M. D., and D. L. Hartmann (2010), Why is longwave cloud feedback positive?, *J. Geophys. Res.*, *115*, D16117, doi:10.1029/2010JD013817.